An extracellular Argonaute protein mediates export of repeat-associated small RNAs into vesicles in parasitic nematodes

Chow FWN[1*], Koutsovoulos G[2,§*], Ovando-Vázquez C[3,§§*], Laetsch DR[2], Bermúdez-Barrientos JR[3], Claycomb JM[4], Blaxter M[2,5**], Abreu-Goodger C[3**], Buck AH[1,5**]

(1) Institute of Immunology and Infection Research, School of Biological Sciences, The University of Edinburgh, Edinburgh EH9 3JT, UK

(2) Institute of Evolutionary Biology, School of Biological Sciences, The University of Edinburgh, Edinburgh EH9 3JT, UK

3) Unidad de Genómica Avanzada (Langebio), Centro de Investigación y de Estudios Avanzados del IPN, Irapuato, Guanajuato 36824, México

(4) Department of Molecular Genetics, University of Toronto, Toronto, ON M5G 1M1, Canada

(5) Centre for Immunity, Infection and Evolution, School of Biological Sciences, The University of Edinburgh, Edinburgh EH9 3JT, UK

§ Current address: INRA, UMR 1355 Institute Sophia Agrobiotech, 06903 Sophia Antipolis, France

§§ Current address: CONACYT-CNS-IPICYT, San Luis Potosí, SLP 78216, México

*Author's contributed equally

**To whom correspondence should be addressed: a.buck@ed.ac.uk, cei.abreu@cinvestav.mx, Mark.Blaxter@ed.ac.uk

Abstract

Mobile small RNAs are an integral component of the arms race between plants and fungal parasites, and several studies suggest microRNAs could similarly operate between parasitic nematodes and their animal hosts. However, whether and how specific sequences are selected for export by parasites is unknown. Here we use density gradient purification and proteinase K sensitivity analysis to demonstrate that a specific Argonaute protein (exWAGO) is secreted in extracellular vesicles (EVs) released by the gastrointestinal nematode *Heligmosomodies bakeri*, at multiple copies per EV. Phylogenetic and gene expression analyses demonstrate exWAGO is highly conserved and abundantly expressed in related parasites, including the human hookworm and proteomic analyses confirm this is the only Argonaute secreted by rodent parasites. In contrast, exWAGO orthologues in species from the free-living genus *Caenorhabditis* are highly diverged. By re-sequencing and re-annotating the *H. bakeri* genome, and sequencing multiple small RNA libraries, we determined that the most abundant small RNAs released from the nematode parasite are not microRNAs but rather secondary small interfering RNAs (siRNAs) that are produced by RNA-dependent RNA Polymerases. We further identify distinct evolutionary properties of the siRNAs resident in free-living or parasitic nematodes versus those exported in EVs by the parasite and show that the latter are specifically associated with exWAGO. Together this work identifies an Argonaute protein as a mediator of RNA export and suggests rhabditomorph nematode parasites may have co-opted a novel nematode-unique pathway to communicate with their hosts.

Introduction

Small RNA-mediated gene regulatory mechanisms are used by cellular organisms and viruses to enable various aspects of their development, defence strategies and physiology (1). In eukaryotes small RNAs (sRNAs) operate within RNA-Induced Silencing Complexes (RISCs). The engines of these complexes are a diverse family of Argonaute proteins that are guided by the sRNA to target nucleic acids in a sequence-specific manner. The downstream effects of sRNA guide-directed recognition are diverse and depend on the biogenesis of the sRNA guide, the class of the target and Argonaute with which they both associate. One deeply conserved sRNA-dependent mechanism is the post-transcriptional regulation of gene expression by microRNAs (miRNAs), which associate with an Argonaute of the AGO clade. MiRNAs were discovered for their crucial roles in development and are now appreciated to regulate numerous aspects of physiology and signalling. In the last 10 years, studies across a broad range of animal systems have implicated miRNAs in intercellular communication through their transport in extracellular vesicles (EVs) (2). Several reports also suggest mammalian miRNAs can move into other organisms, influencing gene expression and growth of microbes in the gut (3) and malaria parasites in the blood (4). We previously reported that the nematode parasite *Heligmosomoides bakeri* (renamed from *Heligmosomoides polygyrus* (5)) releases its own miRNAs within extracellular vesicles (EVs) that are internalized by mouse cells and suppress innate immune responses (6). *H. bakeri* is a natural parasite of mice that serves as an important animal model for the study of immunomodulation by strongylid parasites, which establish chronic infections in their hosts by inducing immune suppression and tolerance. These parasites infect half a billion people and are highly prevalent in livestock. The EVs they release have been shown to be immune suppressive (6, 7), and are targets of protective immunity, suggesting they are important for parasite survival (8, 9).

Our previous proteomic analyses identified one worm (nematode)-specific AGO (WAGO) in the excretory-secretory products and EVs of *H. bakeri*. Here we focus on defining and characterizing the extracellular Argonaute (exWAGO) and exported sRNAs. Nematode pathogens in particular may have evolved a suite of novel RNAi functions based on a unique expansion of Argonaute types (i.e. the WAGOs) (10). The majority of our understanding of nematode RNAi pathways is based on the free-living model organism *Caenorhabditis elegans,* which has at least four types of endogenous sRNAs and 25 Argonaute genes (11). In addition to miRNAs and piRNAs, *C. elegans* produces small interfering RNAs (siRNAs) from exogenous or

84 endogenous double-stranded RNAs (dsRNAs). There is also a mechanism for *de*
85 *novo* generation of siRNAs by RNA-dependent RNA polymerases (RdRPs), which
86 are recruited to sRNA-target transcripts to amplify the silencing signal through the
87 generation of secondary siRNAs. The secondary siRNAs dominate the sRNA
88 content of adult *C. elegans* and have also been documented in several parasitic
89 nematode species (12-15). They are distinguished from other sRNAs by the
90 presence of a 5' triphosphate and a preference for a 5' guanine. In *C. elegans*,
91 secondary siRNAs associate with WAGOs and have been shown to be important in
92 self *versus* non-self-recognition in the germline (16-18). siRNAs can also be
93 transmitted from the soma to the germline to mediate heritable responses to
94 infection and nutrient starvation (19). *C. elegans* therefore sets a precedent for
95 involvement of WAGOs in both defence and environmental adaptation, but the
96 functions of most WAGOs and their siRNA guides remain unknown. Since many
97 nematodes are parasites, and parasitism has arisen multiple times independently
98 (20) it is possible that WAGOs could also contribute to this important lifestyle
99 innovation.

100 Here we examine the molecular and evolutionary properties of exWAGO in
101 parasitic and free-living nematodes and demonstrate that exWAGO mediates the
102 selective export of specific siRNAs in EVs. We compare the genomic origin of
103 siRNAs exported in EVs by *H. bakeri* to the resident siRNAs expressed in adults of
104 both *H. bakeri* and *C. elegans*. Our results support a model where the resident
105 sRNAs are dominated by secondary siRNAs, which are used for endogenous gene
106 regulation and control of retrotransposons. In contrast, the parasite preferentially
107 exports secondary siRNAs that are produced from newly evolved repetitive
108 elements in the genome that associate with exWAGO. This adds evolutionary
109 breadth to the handful of reports in mammalian systems suggesting RNA-binding
110 proteins are a mechanism for selective RNA export (21-23) and establishes *H.*
111 *bakeri* as a tractable model for studying extracellular sRNA biology.
112
113 **Results**
114

115 **A nematode-specific extracellular Argonaute is within extracellular vesicles**
116 **released from *H.bakeri* at several copies per EV**

117 We previously identified an Argonaute protein in the excretory-secretory and EV
118 products of *H. bakeri* based on proteomic analyses (6). Several studies in
119 mammalian systems have similarly reported Argonautes associated with EVs, in

some cases under specific signalling conditions (24). However, Argonautes have also been reported to be contaminants that co-purify with EVs (21). In order to rigorously determine whether the exWAGO that we have identified exists within EVs, we used ultracentrifugation followed by flotation on a sucrose gradient for purification, quantification by nanoparticle tracking analysis and visualisation by transmission electron microscopy. As shown in Figure 1, the EVs had a density of 1.16-1.18 g/cm3 and co-purified with exWAGO. We further subjected the sucrose-purified EV fractions to proteinase K treatment and confirmed that the exWAGO was protected from degradation but became susceptible when the EVs were lysed with detergent (Figure 1D). We analysed a defined number of sucrose-gradient purified EVs by western blot in comparison to recombinant exWAGO and found that exWAGO was present at 3.4 ± 1.1 copies per EV (Figure 1E).

An improved genome assembly and annotation to explore extracellular Argonautes and RNAs

In order to determine the full complement of Argonautes and small RNAs in *H. bakeri* we first generated a new genome assembly for this nematode based on combining short-read (~100-fold read coverage; Illumina) and long-read (~12-fold coverage; PacBio SMRT) data (Supplementary Methods). The final genome assembly spans 697 Mb, 150 Mb longer than the first (Illumina-only) draft (25). While most sequenced nematode genomes are between 60 and 200 Mb, the strongylids (which include *H. bakeri*) tend to have larger genomes, ranging from 170 to 700 Mb (with a mean of ~380 Mb) (25). Our *H. bakeri* assembly is represented by 23,647 contigs (just over half the previous assembly's 44,728 contigs), with an N50 of 180 kb (up from 36 kb). Assessment of genome completeness using the Core Eukaryotic Genes Mapping Approach (CEGMA) and Benchmarking Universal Single-Copy Orthologs (BUSCO) suggests ~88% of conserved genes are complete (~8% partial), with 96% of the assembled *H. bakeri* transcriptome mapping to the genome (Supplemental Table 1). Protein-coding genes were predicted with the BRAKER pipeline generating 23,471 protein-coding genes with 25,215 transcripts. Non-coding RNA genes, including rRNA, tRNA and miRNAs, were predicted using Rfam models and family-specific tools (see Supplementary Methods). The expansion of the *H. bakeri* genome compared to closely related clade V parasites is associated with an expanded repeat content. Over half (58.3%) of the *H. bakeri* genome contains some type of repeat element, including LINE elements (12.6% of the genome) and DNA elements (12.8%) (Table 1). Of all the repeats, 33.3% were found within genes (mostly in introns, which

themselves occupy 33.5% of the genome). Interestingly, 30.6% of the genome was annotated as unclassified repeats, nearly two-thirds of which do not overlap any other kind of annotation.

exWAGO is highly conserved and abundant in rhabditine (Clade V) parasitic nematodes and has diverged in *Caenorhabditis*

To determine the conservation of exWAGO across Clade V nematodes we clustered proteins from the new *H. bakeri* genome with proteomes predicted from the genomes of a selection of rhabditomorph nematodes (including *C. elegans* and six additional *Caenorhabditis* species, eleven strongyle parasites, the entomopathogen *H. bacteriophora*, the free living *Oscheius tipulae*, and the free-living diplogasteromorph *Pristionchus pacificus*) using OrthoFinder (26). The resulting orthogroups were interrogated with Kinfin (27) to identify orthologues of proteins predicted to be involved in RNAi in *H. bakeri* or known to be implicated in RNAi in *C. elegans.* This revealed that, as expected, nearly all of the machinery for miRNA and piRNA pathways, including highly conserved Argonautes ALG-1/2 and PRG1/2, is conserved across Clade V nematodes (Supplemental Figure 1). Previous studies in *C. elegans* have defined populations of primary siRNAs that are 26 nt in length and associated with male or female germline regulation mediated by the Argonautes ALG-3/4 (during spermatogenesis) or ERGO-1 (in oocytes and embryos). Notably ALG-3/4, but not ERGO-1, are conserved in parasites and the general factors associated with 26G RNA biogenesis, also termed the ERI complex (enhanced exogenous RNAi phenotype), are conserved while ERGO-1-specific factors including ERI-6/7/9 and MUT-16 are not (Supplementary Figure 1).

Strikingly, of the thirteen WAGOs in the *C. elegans* gene set, only four had co-clustered orthologues from species other than *Caenorhabditis*. We therefore performed a joint phylogenetic analysis of all orthogroups containing Argonautes (defined by the presence of both PAZ and PIWI domains) (Figure 2A). This identified clades of Argonautes in parasitic species that were sister to *Caenorhabditis*-specific orthogroups. For example, the nuclear WAGOs HRDE-1 and NRDE-3 as well as WAGO-10 and WAGO-11 in *Caenorhabditis* are in fact orthologous to parasite-derived Argonautes in orthogroups OG01747 and OG07955 but their relationship has been obscured by differing rates of evolution in the different species groups. Similarly, the phylogenetic analysis shows that exWAGO does in fact co-cluster with a *Caenorhabditis*-only orthogroup that contains *C. elegans* SAGO-1, SAGO-2 and PPW-1. The orthogroup containing

exWAGO contains Argonautes from many other parasitic strongyles, *H. bacteriophora*, *O. tipulae* and *P. pacificus* as well as Argonautes from *Caenorhabditis* species placed at the base of the genus (*C. monodelphis*, *C. castaneus*, and *C. sp.* 38) (Figure 2B). Examination of the intron-exon structure of these Argonautes supports this relationship (Figure 2C). The most basal *Caenorhabditis*, *C. monodelphis*, has a gene structure very similar to that of the other exWAGOs, but gene structure in other *Caenorhabditis* species has evolved rapidly. We suggest that *C. elegans* SAGO-1, SAGO-2 and PPW-1 are co-orthologues of *H. bakeri* exWAGO, and thus the biology of these genes may illuminate the origins and functions of exWAGO in parasites.

Using our new annotation of Argonautes we used existing RNAseq data to determine the expression levels of all Argonautes in adult life stages of parasitic versus free-living Clade V nematodes. Strikingly, we found that exWAGOs are generally the most abundantly expressed of all Argonautes (Supplementary Table 2), including the sheep parasites *Haemonchus contortus* and *T. circumcinta* and the human hookworm, *Nector americanus* (Figure 3). In contrast, the SAGO-1, 2 and PPW orthologs in *C. elegans* adults are not expressed at high levels (Supplementary Table 2). We further identified exWAGO in the excretory-secretory (ES) products of adult *Nippostrongylus brasiliensis* (another rodent parasite) (Table 1). No peptides mapping to any other Argonaute proteins were identified in multiple samples, pointing to a unique extracellular role for this particular Argonaute across the parasite species.

Comparative analysis of resident sRNA distribution in *H. bakeri* versus *C. elegans* suggests shared functions in endogenous gene regulation

To determine whether the dominance of exWAGO in the parasites was reflected at the level of sRNA composition we first carried out side-by-side analysis of endogenous sRNAs present in *H. bakeri* and *C. elegans* adult nematodes. sRNA datasets were generated in triplicate, capturing either only 5'-monophosphate RNAs or all RNAs (after treatment with 5' polyphosphatase). As expected, the untreated libraries from whole nematodes were dominated by reads mapping to miRNAs in each genome, having the characteristic first nucleotide preference of U and peak length of 22 nt (Figure 4A,D). In contrast, the whole-nematode libraries treated with 5' polyphosphatase showed a clear enrichment for RNAs with a first base preference of guanine, the majority of which were 22 nt in length in *C. elegans* and 23 nt in *H. bakeri* (Figure 4B,E). This signature is characteristic of

secondary siRNA products of RdRPs, and suggests secondary siRNAs dominate the resident sRNA populations of both nematodes. The length variation (22 *versus* 23 nt) may indicate mechanistic differences between the RdRPs that generate them or the Argonaute proteins that stabilize them.

By comparing the 5' polyphosphatase-treated and untreated libraries in both species, we identified 137,531 regions in the *H. bakeri* genome that have more mapped reads from the 5' polyphosphatase-treated libraries (we call these regions polyP-enriched clusters) and 6,075 regions with relatively more reads from the untreated libraries (monoP-enriched clusters, see Methods and Supplemental Figure 2). We reasoned that these represent sRNAs with two distinct modes of biogenesis, with the monoP-enriched clusters containing sRNAs cleaved by ribonucleases (such as Dicer) or being degradation products, and the polyP-enriched clusters containing unprocessed products of RdRPs or RNA polymerase III. Consistent with this model, the monoP-enriched clusters contained a higher fraction of miRNA-mapping reads than the untreated libraries, while the polyP-enriched clusters had a much reduced fraction of miRNA reads (Supplemental Figure 3). The same general strategy was applied to the *C. elegans* sRNAs, to compare the polyP-enriched clusters of both nematodes, which represent by far the most abundant type of sRNA in adults. The majority (62.3%) of the reads within the polyP-enriched clusters of *C. elegans*, mapped antisense to messenger RNAs, consistent with roles in regulating endogenous gene expression (Figure 4C). In contrast, 9.9% of the reads from polyP-enriched clusters of *H. bakeri* mapped antisense to mRNAs (Figure 4F). To compare these numbers, we need to take into account the fraction of each genome occupied by mRNAs. The *C. elegans* genome devotes 28.3% of its base pairs to coding exons (Table 1, Supplemental Figure 4), therefore if sRNAs were produced randomly across the genome 14.1% would map antisense to these. Consequently, our observed proportion of antisense mRNA polyP sRNAs represents a 4.4-fold increase over what is expected by chance. Since only 3.4% of the *H. bakeri* genome encodes exons, the polyP sRNAs that map antisense to mRNAs are 5.8-fold more frequent than expected. Following similar logic, both nematodes have a significant overrepresentation of polyP sRNAs mapping antisense to known retrotransposons (7.4-fold increase in *C. elegans*, 2.5-fold increase in *H. bakeri,* Figure 4C,F). Thus, despite the drastic differences in genome content of the two species, there is a conserved pattern of siRNAs that likely reflect common functionality in endogenous gene regulation and genome defence.

Vesicular siRNAs are largely derived from novel-repeat elements and associate with exWAGO

Our previous work indicated that EVs secreted from *H. bakeri* adults are associated with a population of sRNAs. We characterized miRNAs and Y RNAs, but only sequenced sRNAs with a 5' monophosphate (6). To generate a more comprehensive characterization of EV sRNAs and examine selectivity, we analysed duplicate sRNA datasets from purified EVs, capturing either only 5'-monophosphate RNAs or all RNAs (after treatment with 5' polyphosphatase). To ensure the sequenced sRNAs were derived from EVs, and not co-purifying or free complexes, EVs were purified by ultracentrifugation and sucrose gradient prior to RNA extraction, library preparation and sequencing. We detected several species of miRNA in EV-derived libraries as expected from our previous work, however the vast majority of EV sRNAs are 23G siRNAs, only detected with 5' polyphosphatase treatment (Figure 4H). To focus on the RdRP products, we selected the polyP-enriched clusters (Supplemental Figure 2). EV-derived, polyP-enriched sRNAs had a 1.9-fold enrichment for siRNAs derived from transposons and a 1.7-fold enrichment for species-specific repeats of the *H. bakeri* genome, compared to the polyP-enriched sRNAs from adults (Figure 4I). In contrast, the siRNAs mapping antisense to protein coding genes and retrotransposons were relatively depleted within the EV libraries. These results suggest selective partitioning of siRNA biotypes into the EVs and identifies recently evolved regions of the genome as a primary source of EV sRNA.

To further explore and quantify this selectivity, we calculated, for each polyP-enriched cluster, a measure of entropy-based Information Content (IC) using either adult or EV reads (see Methods). The higher the IC value, the more concentrated the reads are in a few peaks, while the lower the IC value, the more evenly distributed the reads are across the cluster (e.g. Figure 5A, inset). Interestingly, the IC values are consistently higher for reads coming from EVs than from adult libraries (Figure 5A), indicating that the EVs more often contain reads from specific peaks and are not a random sampling of the adult sRNA pool. Figure 5B illustrates a region in the *H. bakeri* genome that produces siRNAs enriched in the EVs. The only annotated elements in this region are repeats, mostly novel (species-specific) elements. These results support the idea that EV content reflects a selection of specific siRNA sequences.

296 To determine whether exWAGO specifically associates with the EV-enriched
297 sRNAs produced from novel repeats, we immunoprecipitated the adult nematode
298 lysates using an antibody raised against exWAGO and analysed by qRT-PCR the
299 co-purified sRNAs. The siRNAs that derive from EV-enriched clusters
300 immunopurified with exWAGO and were depleted in the unbound fraction (Figure
301 6). We observed the opposite pattern with the IgG bead control. In contrast,
302 siRNAs derived from selected clusters that are abundant in adults but not
303 represented in the EVs did not copurify with exWAGO, nor did Y RNAs or a
304 conserved miRNA (Figure 6). These results suggest that specific siRNA sequences
305 bind to exWAGO, which mediates their encapsulation in EVs and defines the
306 population of vesicular sRNAs that are secreted into the host environment.

307 **Discussion**
308
309 That small RNAs are transferred within organisms, and between organisms, has
310 many implications in cross-species communication and disease. However, there
311 are many questions regarding how RNAs are selected for export from the donor,
312 which RNAs are transferred to the recipient, and whether and how these RNAs
313 function within the recipient. Here we have examined the question of the specificity
314 of packaging of sRNAs in EVs in the model parasite *H. bakeri* using comparative
315 analyses of the origin of sRNAs within the body of the nematode *versus* those
316 selected to be exported in EVs. We compare this to evolutionary analyses of the
317 sRNA machinery in the parasite and the closely related, free-living *C. elegans*. We
318 find that secondary siRNAs within adults of both the free-living and the parasitic
319 nematodes are largely produced to target mRNAs and retrotransposons by
320 antisense pairing along their entire length, and are therefore associated with
321 endogenous gene regulation and defence. In contrast the siRNAs within EVs
322 secreted by the parasite do not appear to be a stochastic sampling of those
323 detected in the adult nematodes but are specifically enriched for those produced
324 from transposons and newly-evolved, repetitive regions in the genome. This
325 suggests both mechanistic and evolutionary selectivity.

326 Our immunoprecipitation experiments show that Y RNAs, which are also abundant
327 in EVs (6), do not associate with exWAGO, suggesting this protein is specific for
328 siRNAs. Mechanistically, we envision three processes that could contribute to the
329 total RNA present in EVs, acting independently or together. The EVs could be
330 passively loaded with the sRNAs present in the cell type from which EVs are
331 exported. It is likely that EVs are released from the intestine (6). Secondly, the

sRNAs could be actively loaded by some intrinsic property, perhaps related to their specific biogenesis pathway. Lastly, the sRNAs could associate with a specific RNA-binding protein, as has been shown in some mammalian systems. Our immunoprecipitation data suggest that associative binding occurs for the siRNAs and we identify exWAGO as the mediator of this selective export. Intriguingly exWAGO is highly conserved and abundant in all Clade V parasitic nematodes examined, and we have further shown that it is also secreted in the rodent parasitic nematode *N.brasiliensis*. We propose therefore that the mechanism of exWAGO-mediated siRNA export extends beyond the *H. bakeri* model.

The sRNAs selected for export with exWAGO derive from regions of the *H. bakeri* genome that are repetitive and novel, which may reflect recent, dynamic evolution of this putative host manipulation system. Rather than derive sRNAs from conserved loci, and risk self-directed effects, selection may exploit the rapidly evolving non-genic portion of the genome to generate evolutionarily novel but host-relevant sRNA loci. It will be informative to correlate these sequences with host genes and to explore their evolution across parasites.

We identified the SAGO and PPW proteins in *C. elegans* and related *Caenorhabditis* species as diverged exWAGO orthologues. Although as yet we have no evidence that the SAGOs (or any other AGOs) are exported extra-organismally from *C. elegans,* preliminary data suggest these may both have common localization in the intestine ((6) and Claycomb, Seroussi, unpublished). It will be of interest to understand whether SAGO and PPW function within *C. elegans* can shed light on the roles of exWAGO.

Very little is understood regarding the evolution of cross-species communication. That pathogens use small RNAs to modulate their hosts is not unexpected, as it has been well documented in interactions between parasitic fungi and plants (28) and it is similar, conceptually, to the evolution of miRNAs in certain viruses (29). In contrast to viruses, however, extracellular parasites such as *H. bakeri* require a mechanism for transporting specific sRNAs into host cells. The packaging of siRNAs in EVs by exWAGO provides such a mechanism. Notably, EVs have recently been implicated in the transfer of RNA in plants, in this case from the plant cells to fungal parasites (30). We do not yet know if exWAGO is solely involved in export, or is also involved in mediating functional effects inside the recipient cells. Further work is required to understand the individual and collective contributions of all of the EV cargos in host cell modulation. This work establishes a parasite

Argonaute as a sorting mechanism for EV RNAs, indicates that focusing only on miRNAs can be misleading and provides an important framework for interrogating new parasite-host interactions and their consequences on infection.

Materials and Methods are provided in Supplementary Material.

Acknowledgements

This work was supported by HFSP grant RGY0069 to AB, CA and JC. We thank Elaine Robertson for technical support for the *H. bakeri* life cycle, Sujai Kumar for support with genome analysis, Tuhin Maity for preparation of *C. elegans* samples and Rick Maizels for ES from *N. brasiliensis*.

Competing interests

The authors declare no competing interests.

Figure legends

Figure 1: exWAGO is vesicular and present at multiple copies per EV

A) Western blot analysis of equal volumes of sucrose-gradient fractions of EVs from *H. bakeri* using antibody against exWAGO, B) Silver stain blot of same fractions, C) Nanoparticle tracking analysis of EV total number in each fraction (left) and TEM of 1.16 g/cm3 fraction (right). D) Western blot of exWAGO from gradient-purified EVs and following treatment with Proteinase K (5 ug/mL) with or without Triton-X (0.05%). E) Western blot of 3 independent biological replicates of sucrose-gradient purified *H. bakeri* EVs, using recombinant standard of exWAGO for quantification.

Figure 2: Phylogenetic tree of Argonautes in Clade V nematodes and gene structure of exWAGO. A) Grey shading denotes different orthogroups, *C. elegans* protein names in each clade are noted (or absent if no orthologues in that Clade). B) Tree showing phylogenetic relationship and branch lengths of exWAGO orthologues across Clade V, C) Conservation of exons and introns in exWAGO homologues. Each box is an exon with the width denoting length. Boxes with dashed lines denote exons with possible errors in the genome assembly of the species. Colours denote differences in exon size in triplets compared to exWAGO.

Figure 3: Expression of Argonautes across Clade V parasitic nematodes Relative expression levels of Argonautes from RNAseq data of the adult parasites noted. Data were based on the sum of tpm reads for each orthogroup (defined in Figure 2), normalized to tpm for OG1273 orthogroup (ALG-1/2). The total number of distinct transcripts in each orthogroup in each species is noted below each

column. The known *C.elegans* Argonaute names are used where applicable, or exWAGO as defined in this work.

Figure 4: sRNA composition in adult *C. elegans* and *H. bakeri*, compared to *H. bakeri* extracellular vesicles. First nucleotide and length distribution of untreated small RNA libraries for *C. elegans* adults (A), *H. bakeri* adults (D) and *H. bakeri* EVs (G), and their corresponding polyphosphatase-treated libraries (B,E,H). The proportions of the 20-25 nt reads mapping within annotated categories in the genome (from Table 1) are shown beneath each barplot. Line plots for *C. elegans* (C) and *H. bakeri* (F) showing the relationship between the percentage of the genome occupied by each annotation category and the percentage of 20-25 nt reads from the polyP-enriched clusters, while (I) shows the relationship between the percentage of the 20-25 nt reads from the adult polyP-enriched clusters to those from the EV polyP-enriched clusters (see Methods).

Figure 5: Clusters with transposons or novel repeats have higher Information Content in extracellular vesicles than in adults. Dot plot comparing Counts Per Million and Information Content of all clusters with transposons or novel repeats (A). Top and side barplots show the number of clusters at each value of the X or Y-axis respectively. Inset: example of read coverage for cluster ncRNA_44089. Read coverage (top), annotation of repeat elements (middle) and zoomed-in read coverage (bottom, in $\log_2$-scale to distinguish individual libraries) for the most highly expressed cluster in EVs (B). In all cases blue indicates EV and red indicates Adult libraries.

Figure 6: Immunoprecipitation of exWAGO and detection of associated sequences. A) Western blot to detect exWAGO following immunoprecipitation of 10 ug adult worm lysates with exWAGO anti sera or control (naïve) sera. Equivalent volumes input and unbound were loaded (unbound is defined as first flow-through from beads). B) qRT-PCR analysis of samples from (A) for siRNAs derived from EV-enriched or adult-enriched clusters as well as Y-RNA and miR-100. To ensure equivalent recovery of RNA, a synthetic spike was included prior to extraction which varied <2 fold across all sample types. Data are shown as mean with standard deviation for n=3.

Supplementary Figure 1 Conservation of RNAi pathway in Clade V

Presence or absence of orthologues to *C. elegans* genes associated with RNAi pathways in Clade V organisms. Phylogenetic relationship is shown at the top of table, gene identities across each species are detailed in https://github.com/DRL/chow2018.

Supplementary Figure 2: Expression of all sRNA clusters (dots) comparing the average counts-per-million (X-axis) to the fold-change of polyphosphatase-treated relative to untreated libraries (Y-axis). Blue and red dots highlight those clusters identified respectively as polyP (enriched in polyphosphatase treated libraries) or monoP (similar normalised expression between treated and untreated libraries) for *C. elegans* adult nematodes (A), and *H. bakeri* adults (B) or extracellular vesicles (C). Clusters containing known miRNAs (expected to be monoP) are highlighted in gold.

Supplementary Figure 3: Distribution of reads in annotated categories for each type of library, comparing the reads falling within monoP or polyP clusters to all reads. Plots are shown for untreated libraries for *C. elegans* (A) and *H. bakeri* (B), and polyphosphatase-treated libraries for *C. elegans* (C) and *H. bakeri* (D).

Supplementary Figure 4: Comparison of *C. elegans* and *H. bakeri* genome sizes and fractions of each genome devoted to annotated.

Supplementary Table 1: New *H.bakeri* genome assembly information

Supplementary Table 2: Details of RNAseq data used for Figure 3

465 **Table 1. Non-overlapping genome composition**

	C. elegans		*H. bakeri*	
	bases	%	*bases*	%
intergenic	29,355,343	29.272	168,174,849	24.130
exons	28,409,938	28.329	23,682,169	3.398
introns	25,956,467	25.882	170,798,580	24.506
transposons	11,880,919	11.847	92,998,044	13.343
novel repeats	1,402,898	1.399	13,1452,375	18.861
retroelements	1,307,772	1.304	104,917,538	15.054
satellite repeats	594,478	0.593	377,947	0.054
simple repeats	581,880	0.580	2,960,599	0.425
other ncRNA	429,956	0.429	749,784	0.108
piRNA	256,574	0.256	63,990	0.009
tRNA	62,284	0.062	675,650	0.097
miRNA	35,312	0.035	43,955	0.006
rRNA	9,520	0.009	53,983	0.008
yRNA	3,060	0.003	5,940	0.001
TOTAL	100,286,401	100%	696,955,403	100%

466

467 **Table 2. ExWAGO identified in EV products by mass spectrometry**

Species	Protein	Accession number	Length (aa)	Predicted MW (kDa)	Predicted PI	Unique peptide sequence (Start position)
H. bakeri	exWAGO	HPOL_0000298601-mRNA-1	912	102	9.23	TGMGQLSVGAVALPEKR (6) SAAVAVYK (86) AAVLFSAQR (114) QFMLPASVVSSAGPDATGIR (132) ISQMSIFFDQR (277) NAMQPFNQK (297) VTLQQQTPDQVASMIK (393) ASATLPQTR (409) IMKDALDITPR (423) AATTIAPR (716) LVNDGDLK (899)
N. brasiliensis	exWAGO	NBR_exWAGO	913	102	9.25	QDFVCNLTALK (32) DIFPQDSALFYDR (102) ILPTPTILYGER (457)

References

1. Swarts DC, *et al.* (2014) The evolutionary journey of Argonaute proteins. *Nature structural & molecular biology* 21(9):743-753.
2. Tkach M & Thery C (2016) Communication by Extracellular Vesicles: Where We Are and Where We Need to Go. *Cell* 164(6):1226-1232.
3. Liu S, *et al.* (2016) The Host Shapes the Gut Microbiota via Fecal MicroRNA. *Cell host & microbe* 19(1):32-43.
4. LaMonte G, *et al.* (2012) Translocation of sickle cell erythrocyte microRNAs into Plasmodium falciparum inhibits parasite translation and contributes to malaria resistance. *Cell host & microbe* 12(2):187-199.
5. Behnke JM, Menge DM, & Noyes H (2009) Heligmosomoides bakeri: a model for exploring the biology and genetics of resistance to chronic gastrointestinal nematode infections. *Parasitology* 136(12):1565-1580.
6. Buck AH, *et al.* (2014) Exosomes secreted by nematode parasites transfer small RNAs to mammalian cells and modulate innate immunity. *Nature communications* 5:5488.
7. Eichenberger RM, *et al.* (2018) Hookworm Secreted Extracellular Vesicles Interact With Host Cells and Prevent Inducible Colitis in Mice. *Frontiers in immunology* 9:850.
8. Coakley G, *et al.* (2017) Extracellular Vesicles from a Helminth Parasite Suppress Macrophage Activation and Constitute an Effective Vaccine for Protective Immunity. *Cell reports* 19(8):1545-1557.
9. Shears RK, Bancroft AJ, Hughes GW, Grencis RK, & Thornton DJ (2018) Extracellular vesicles induce protective immunity against Trichuris muris. *Parasite immunology*:e12536.
10. Buck AH & Blaxter M (2013) Functional diversification of Argonautes in nematodes: an expanding universe. *Biochemical Society transactions* 41(4):881-886.
11. Youngman EM & Claycomb JM (2014) From early lessons to new frontiers: the worm as a treasure trove of small RNA biology. *Frontiers in genetics* 5:416.
12. Holz A & Streit A (2017) Gain and Loss of Small RNA Classes-Characterization of Small RNAs in the Parasitic Nematode Family Strongyloididae. *Genome biology and evolution* 9(10):2826-2843.
13. Pak J & Fire A (2007) Distinct populations of primary and secondary effectors during RNAi in C. elegans. *Science* 315(5809):241-244.
14. Sarkies P, *et al.* (2015) Ancient and novel small RNA pathways compensate for the loss of piRNAs in multiple independent nematode lineages. *PLoS biology* 13(2):e1002061.
15. Yigit E, *et al.* (2006) Analysis of the C. elegans Argonaute family reveals that distinct Argonautes act sequentially during RNAi. *Cell* 127(4):747-757.
16. Ashe A, *et al.* (2012) piRNAs can trigger a multigenerational epigenetic memory in the germline of C. elegans. *Cell* 150(1):88-99.
17. Lee HC, *et al.* (2012) C. elegans piRNAs mediate the genome-wide surveillance of germline transcripts. *Cell* 150(1):78-87.
18. Shirayama M, *et al.* (2012) piRNAs initiate an epigenetic memory of nonself RNA in the C. elegans germline. *Cell* 150(1):65-77.
19. Rechavi O & Lev I (2017) Principles of Transgenerational Small RNA Inheritance in Caenorhabditis elegans. *Current biology : CB* 27(14):R720-R730.
20. Blaxter ML, *et al.* (1998) A molecular evolutionary framework for the phylum Nematoda. *Nature* 392(6671):71-75.

21. Shurtleff MJ, Temoche-Diaz MM, Karfilis KV, Ri S, & Schekman R (2016) Y-box protein 1 is required to sort microRNAs into exosomes in cells and in a cell-free reaction. *eLife* 5.
22. Santangelo L*, et al.* (2016) The RNA-Binding Protein SYNCRIP Is a Component of the Hepatocyte Exosomal Machinery Controlling MicroRNA Sorting. *Cell reports* 17(3):799-808.
23. Villarroya-Beltri C*, et al.* (2013) Sumoylated hnRNPA2B1 controls the sorting of miRNAs into exosomes through binding to specific motifs. *Nature communications* 4:2980.
24. McKenzie AJ*, et al.* (2016) KRAS-MEK Signaling Controls Ago2 Sorting into Exosomes. *Cell reports* 15(5):978-987.
25. Consortium IHG (2018) Comparative genomics of the major parasitic worms. *bioRxiv* 36539; doi: https://doi.org/10.1101/236539.
26. Emms DM & Kelly S (2015) OrthoFinder: solving fundamental biases in whole genome comparisons dramatically improves orthogroup inference accuracy. *Genome biology* 16:157.
27. Laetsch DR & Blaxter ML (2017) KinFin: Software for Taxon-Aware Analysis of Clustered Protein Sequences. *G3* 7(10):3349-3357.
28. Weiberg A*, et al.* (2013) Fungal small RNAs suppress plant immunity by hijacking host RNA interference pathways. *Science* 342(6154):118-123.
29. Pfeffer S*, et al.* (2004) Identification of virus-encoded microRNAs. *Science* 304(5671):734-736.
30. Cai Q*, et al.* (2018) Plants send small RNAs in extracellular vesicles to fungal pathogen to silence virulence genes. *Science* 360(6393):1126-1129.

Figure 1

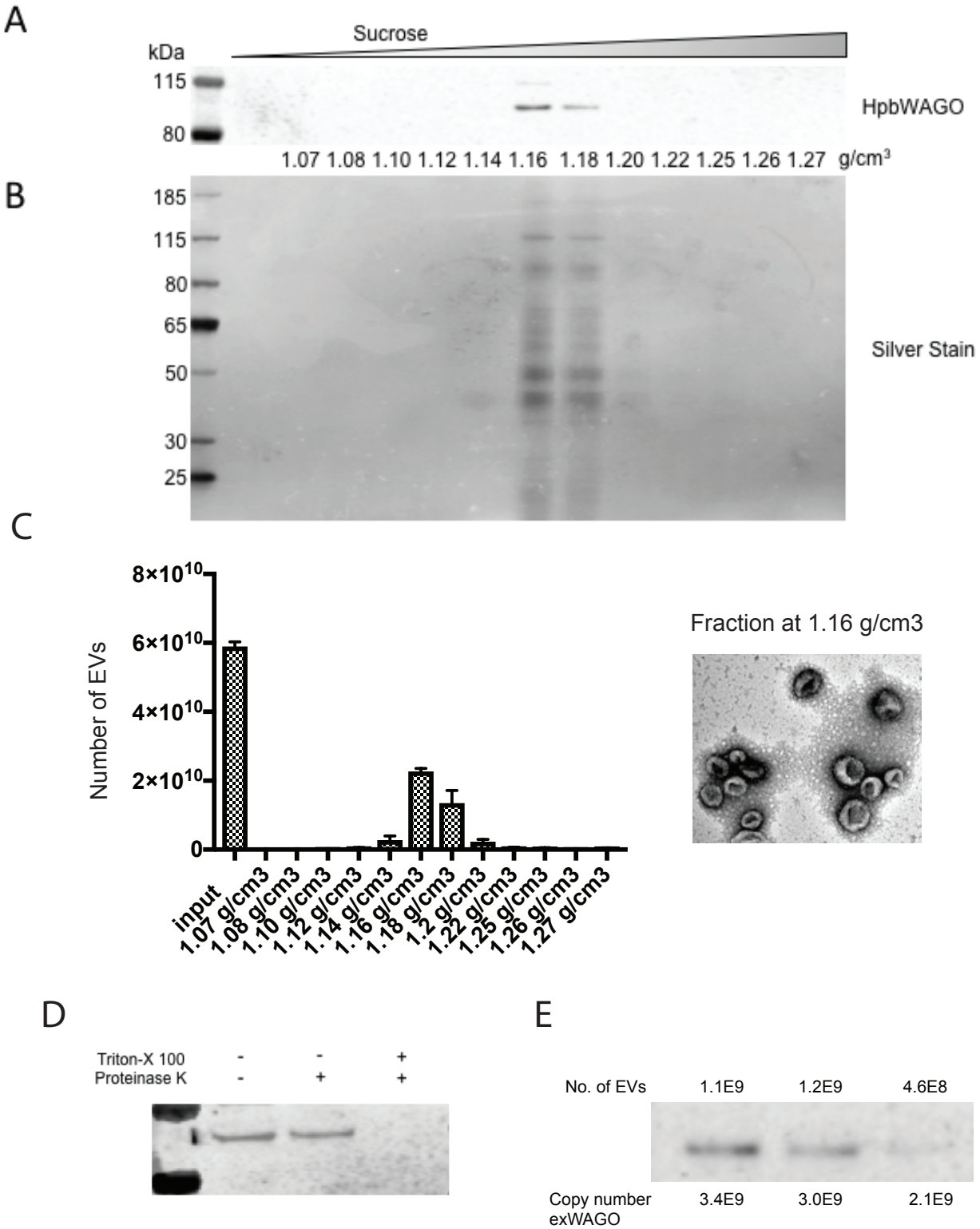

Figure 2

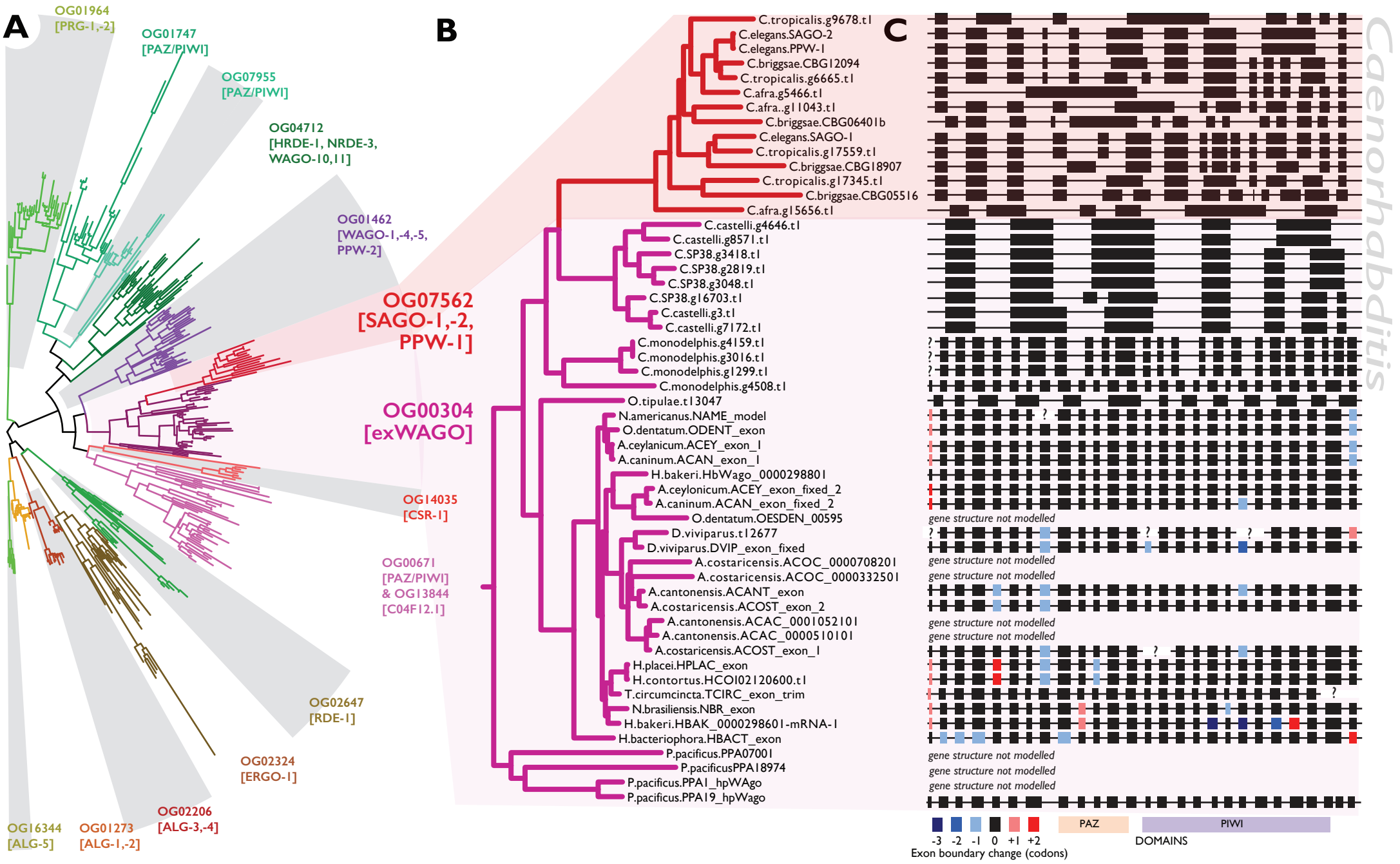
A
OG01964
[PRG-1,-2]
OG01747
[PAZ/PIWI]
OG07955
[PAZ/PIWI]
OG04712
[HRDE-1, NRDE-3,
WAGO-10,11]
OG01462
[WAGO-1,-4,-5,
PPW-2]
OG07562
[SAGO-1,-2,
PPW-1]
OG00304
[exWAGO]
OG14035
[CSR-1]
OG00671
[PAZ/PIWI]
& OG13844
[C04F12.1]
OG02647
[RDE-1]
OG02324
[ERGO-1]
OG02206
[ALG-3,-4]
OG16344
[ALG-5]
OG01273
[ALG-1,-2]
B
C.tropicalis.g9678.t1
C.elegans.SAGO-2
C.elegans.PPW-1
C.briggsae.CBG12094
C.tropicalis.g6665.t1
C.afra.g5466.t1
C.afra..g11043.t1
C.briggsae.CBG06401b
C.elegans.SAGO-1
C.tropicalis.g17559.t1
C.briggsae.CBG18907
C.tropicalis.g17345.t1
C.briggsae.CBG05516
C.afra.g15656.t1
C.castelli.g4646.t1
C.castelli.g8571.t1
C.SP38.g3418.t1
C.SP38.g2819.t1
C.SP38.g3048.t1
C.SP38.g16703.t1
C.castelli.g3.t1
C.castelli.g7172.t1
C.monodelphis.g4159.t1
C.monodelphis.g3016.t1
C.monodelphis.g1299.t1
C.monodelphis.g4508.t1
O.tipulae.t13047
N.americanus.NAME_model
O.dentatum.ODENT_exon
A.ceylanicum.ACEY_exon_1
A.caninum.ACAN_exon_1
H.bakeri.HbWago_0000298801
A.ceylonicum.ACEY_exon_fixed_2
A.caninum.ACAN_exon_fixed_2
O.dentatum.OESDEN_00595
D.viviparus.t12677
D.viviparus.DVIP_exon_fixed
A.costaricensis.ACOC_0000708201
A.costaricensis.ACOC_0000332501
A.cantonensis.ACANT_exon
A.costaricensis.ACOST_exon_2
A.cantonensis.ACAC_0001052101
A.cantonensis.ACAC_0000510101
A.costaricensis.ACOST_exon_1
H.placei.HPLAC_exon
H.contortus.HCOI02120600.t1
T.circumcincta.TCIRC_exon_trim
N.brasiliensis.NBR_exon
H.bakeri.HBAK_0000298601-mRNA-1
H.bacteriophora.HBACT_exon
P.pacificus.PPA07001
P.pacificusPPA18974
P.pacificus.PPA1_hpWAgo
P.pacificus.PPA19_hpWago
C
Caenorhabditis
gene structure not modelled
gene structure not modelled
gene structure not modelled
gene structure not modelled
gene structure not modelled
gene structure not modelled
PAZ
PIWI
-3 -2 -1 0 +1 +2
Exon boundary change (codons)
DOMAINS

Figure 3

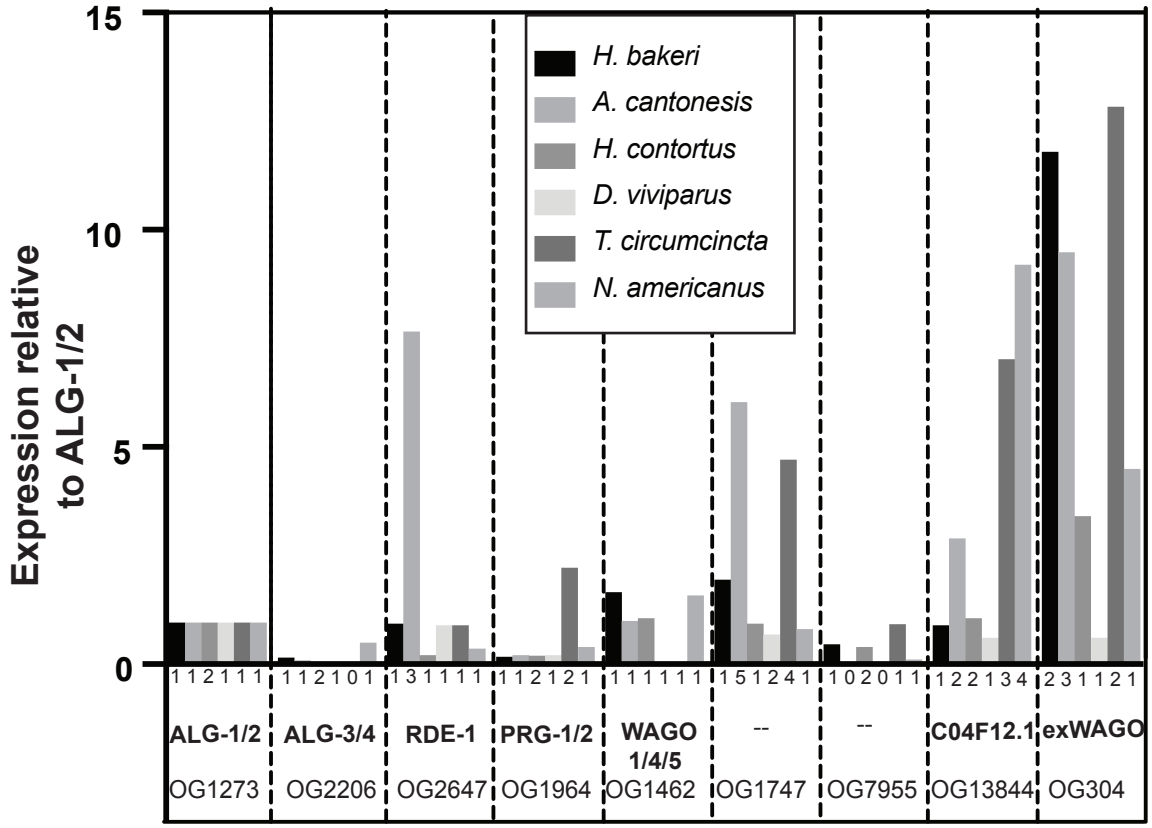

Figure 4

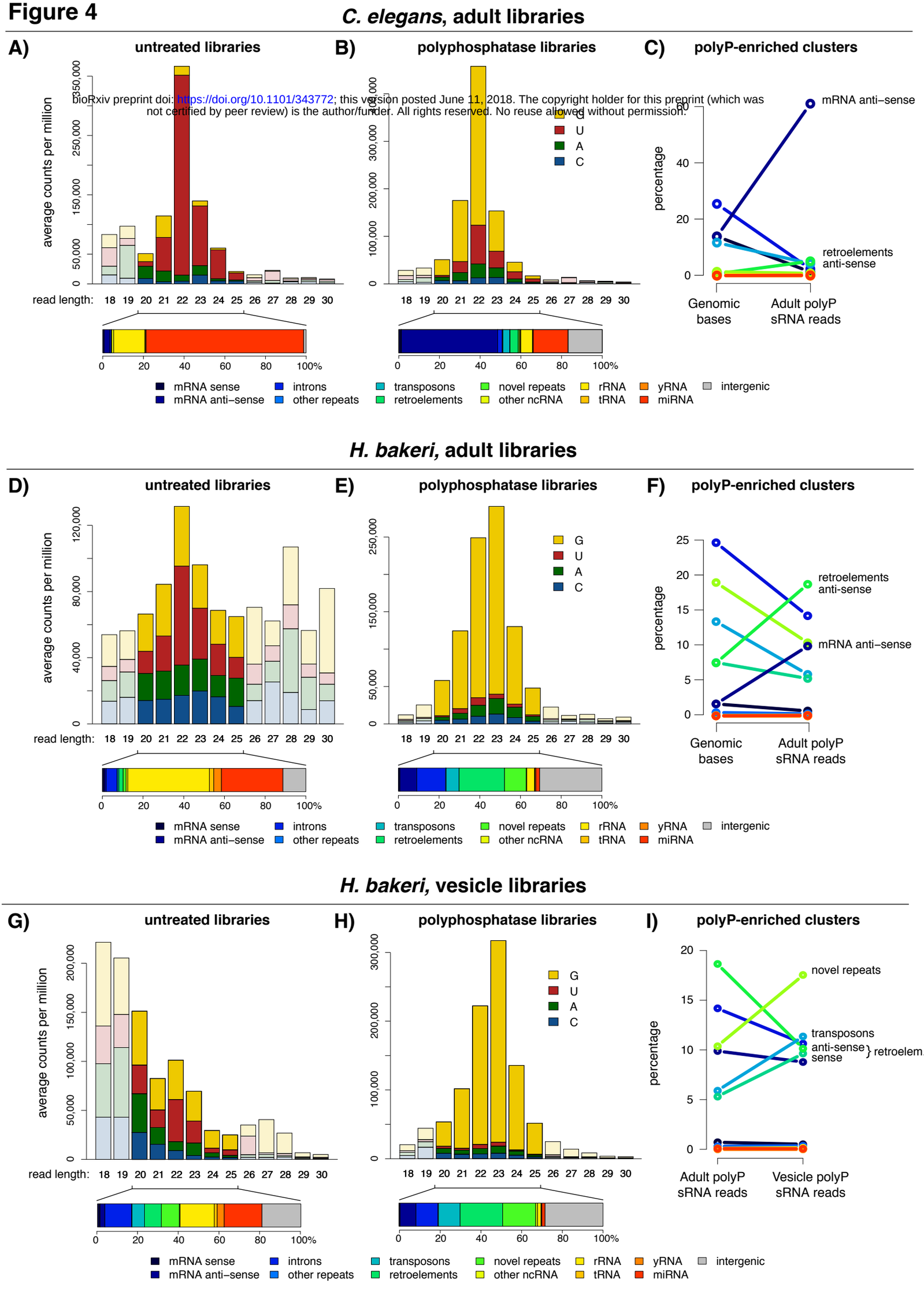

Figure 5

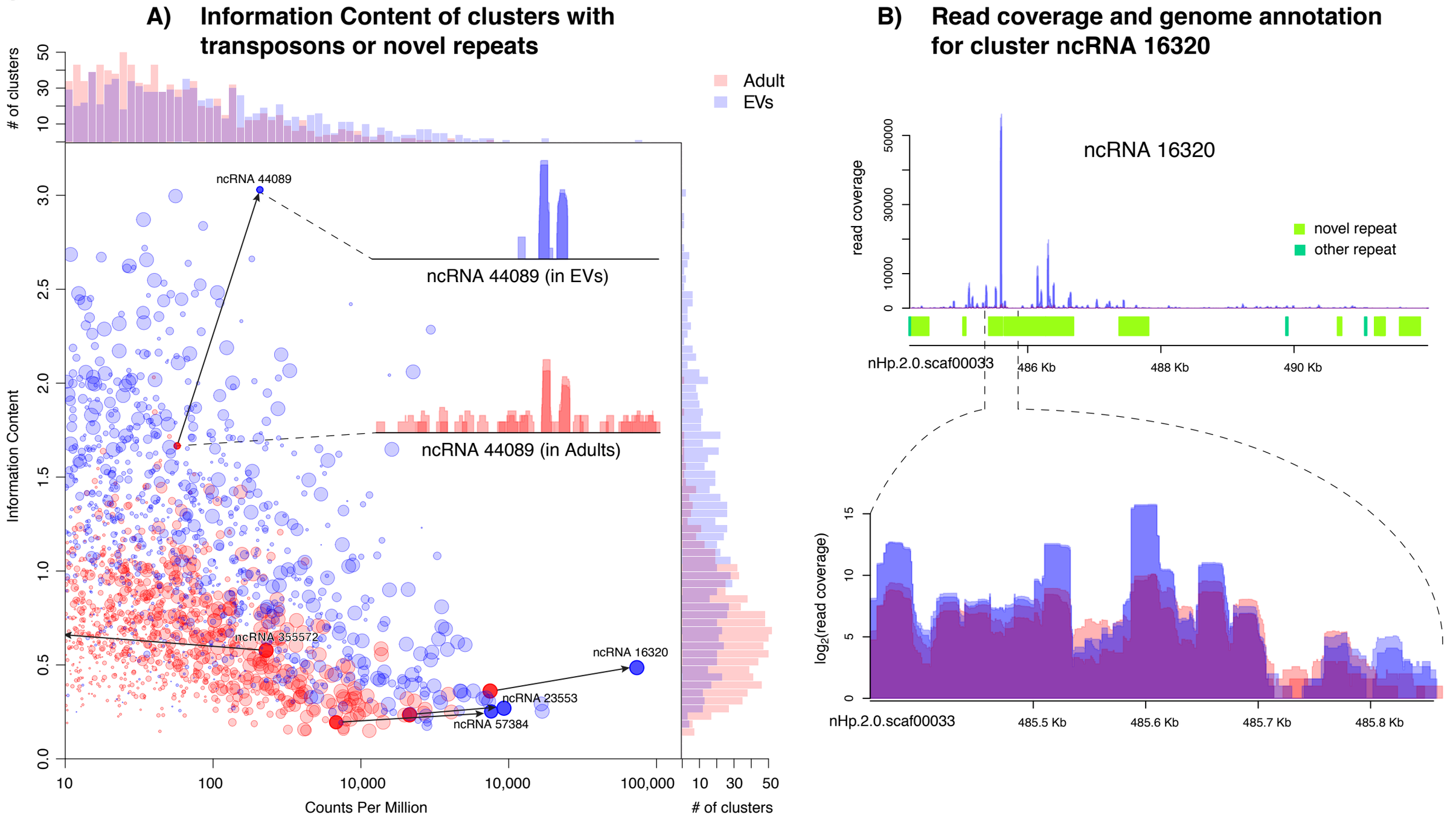
A) Information Content of clusters with transposons or novel repeats
Adult
EVs
# of clusters
Information Content
Counts Per Million
ncRNA 44089
ncRNA 44089 (in EVs)
ncRNA 44089 (in Adults)
ncRNA 355572
ncRNA 16320
ncRNA 23553
ncRNA 57384
B) Read coverage and genome annotation for cluster ncRNA 16320
ncRNA 16320
read coverage
novel repeat
other repeat
nHp.2.0.scaf00033
486 Kb
488 Kb
490 Kb
log2(read coverage)
485.5 Kb
485.6 Kb
485.7 Kb
485.8 Kb

Figure 6

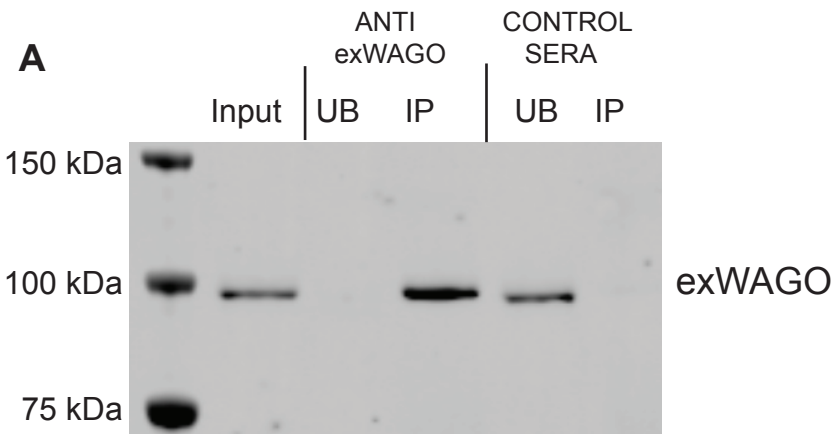

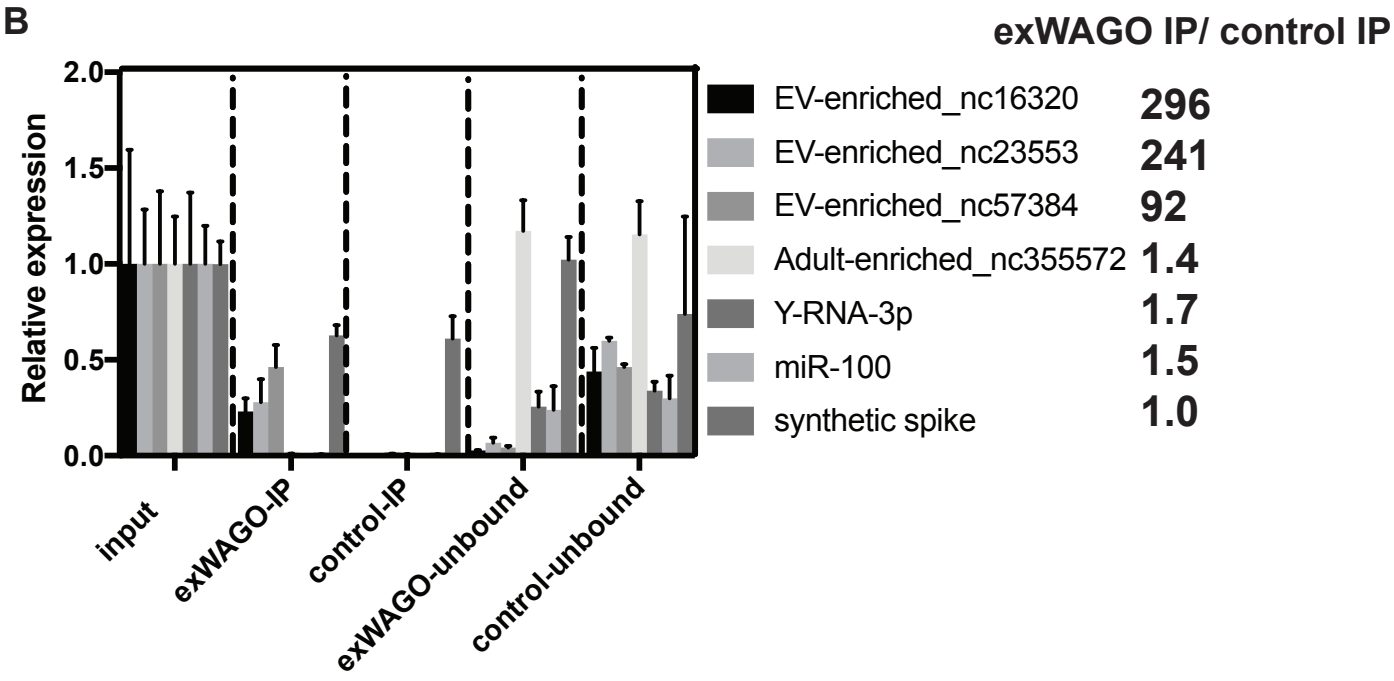

Supplementary Figure 1

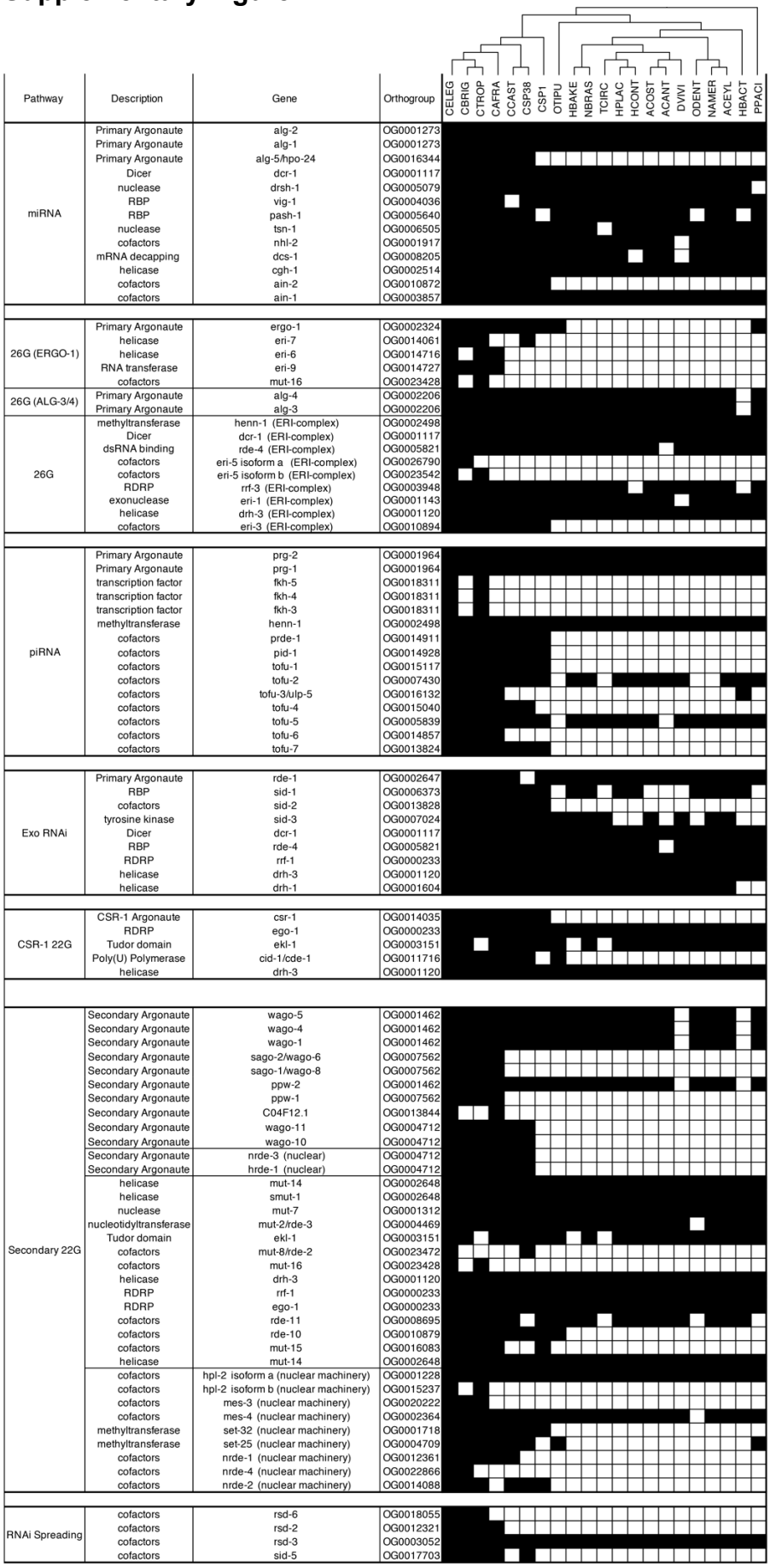

Pathway	Description	Gene	Orthogroup
miRNA	Primary Argonaute	alg-2	OG0001273
	Primary Argonaute	alg-1	OG0001273
	Primary Argonaute	alg-5/hpo-24	OG0016344
	Dicer	dcr-1	OG0001117
	nuclease	drsh-1	OG0005079
	RBP	vig-1	OG0004036
	RBP	pash-1	OG0005640
	nuclease	tsn-1	OG0006505
	cofactors	nhl-2	OG0001917
	mRNA decapping	dcs-1	OG0008205
	helicase	cgh-1	OG0002514
	cofactors	ain-2	OG0010872
	cofactors	ain-1	OG0003857
26G (ERGO-1)	Primary Argonaute	ergo-1	OG0002324
	helicase	eri-7	OG0014061
	helicase	eri-6	OG0014716
	RNA transferase	eri-9	OG0014727
	cofactors	mut-16	OG0023428
26G (ALG-3/4)	Primary Argonaute	alg-4	OG0002206
	Primary Argonaute	alg-3	OG0002206
26G	methyltransferase	henn-1 (ERI-complex)	OG0002498
	Dicer	dcr-1 (ERI-complex)	OG0001117
	dsRNA binding	rde-4 (ERI-complex)	OG0005821
	cofactors	eri-5 isoform a (ERI-complex)	OG0026790
	cofactors	eri-5 isoform b (ERI-complex)	OG0023542
	RDRP	rrf-3 (ERI-complex)	OG0003948
	exonuclease	eri-1 (ERI-complex)	OG0001143
	helicase	drh-3 (ERI-complex)	OG0001120
	cofactors	eri-3 (ERI-complex)	OG0010894
piRNA	Primary Argonaute	prg-2	OG0001964
	Primary Argonaute	prg-1	OG0001964
	transcription factor	fkh-5	OG0018311
	transcription factor	fkh-4	OG0018311
	transcription factor	fkh-3	OG0018311
	methyltransferase	henn-1	OG0002498
	cofactors	prde-1	OG0014911
	cofactors	pid-1	OG0014928
	cofactors	tofu-1	OG0015117
	cofactors	tofu-2	OG0007430
	cofactors	tofu-3/ulp-5	OG0016132
	cofactors	tofu-4	OG0015040
	cofactors	tofu-5	OG0005839
	cofactors	tofu-6	OG0014857
	cofactors	tofu-7	OG0013824
Exo RNAi	Primary Argonaute	rde-1	OG0002647
	RBP	sid-1	OG0006373
	cofactors	sid-2	OG0013828
	tyrosine kinase	sid-3	OG0007024
	Dicer	dcr-1	OG0001117
	RBP	rde-4	OG0005821
	RDRP	rrf-1	OG0000233
	helicase	drh-3	OG0001120
	helicase	drh-1	OG0001604
CSR-1 22G	CSR-1 Argonaute	csr-1	OG0014035
	RDRP	ego-1	OG0000233
	Tudor domain	ekl-1	OG0003151
	Poly(U) Polymerase	cid-1/cde-1	OG0011716
	helicase	drh-3	OG0001120
Secondary 22G	Secondary Argonaute	wago-5	OG0001462
	Secondary Argonaute	wago-4	OG0001462
	Secondary Argonaute	wago-1	OG0001462
	Secondary Argonaute	sago-2/wago-6	OG0007562
	Secondary Argonaute	sago-1/wago-8	OG0007562
	Secondary Argonaute	ppw-2	OG0001462
	Secondary Argonaute	ppw-1	OG0007562
	Secondary Argonaute	C04F12.1	OG0013844
	Secondary Argonaute	wago-11	OG0004712
	Secondary Argonaute	wago-10	OG0004712
	Secondary Argonaute	nrde-3 (nuclear)	OG0004712
	Secondary Argonaute	hrde-1 (nuclear)	OG0004712
	helicase	mut-14	OG0002648
	helicase	smut-1	OG0002648
	nuclease	mut-7	OG0001312
	nucleotidyltransferase	mut-2/rde-3	OG0004469
	Tudor domain	ekl-1	OG0003151
	cofactors	mut-8/rde-2	OG0023472
	cofactors	mut-16	OG0023428
	helicase	drh-3	OG0001120
	RDRP	rrf-1	OG0000233
	RDRP	ego-1	OG0000233
	cofactors	rde-11	OG0008695
	cofactors	rde-10	OG0010879
	cofactors	mut-15	OG0016083
	helicase	mut-14	OG0002648
	cofactors	hpl-2 isoform a (nuclear machinery)	OG0001228
	cofactors	hpl-2 isoform b (nuclear machinery)	OG0015237
	cofactors	mes-3 (nuclear machinery)	OG0020222
	cofactors	mes-4 (nuclear machinery)	OG0002364
	methyltransferase	set-32 (nuclear machinery)	OG0001718
	methyltransferase	set-25 (nuclear machinery)	OG0004709
	cofactors	nrde-1 (nuclear machinery)	OG0012361
	cofactors	nrde-4 (nuclear machinery)	OG0022866
	cofactors	nrde-2 (nuclear machinery)	OG0014088
RNAi Spreading	cofactors	rsd-6	OG0018055
	cofactors	rsd-2	OG0012321
	cofactors	rsd-3	OG0003052
	cofactors	sid-5	OG0017703

Supplemental Figure 2

A) *C. elegans* Adult libs, monoP and polyP-enriched clusters

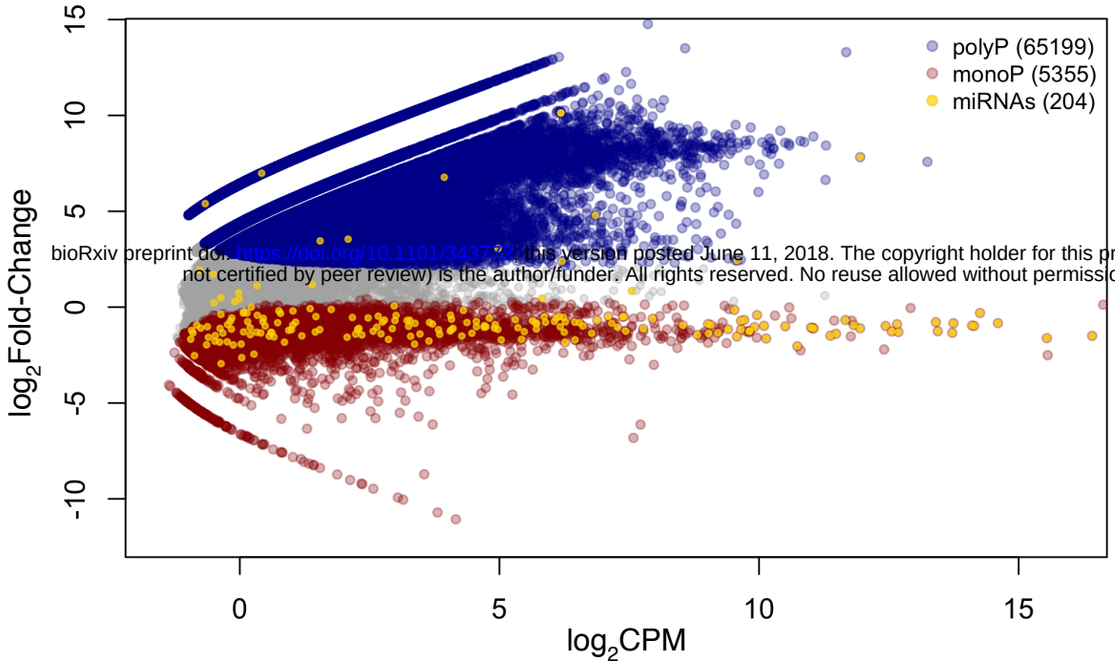

B) *H. bakeri* Adult libs, monoP and polyP-enriched clusters

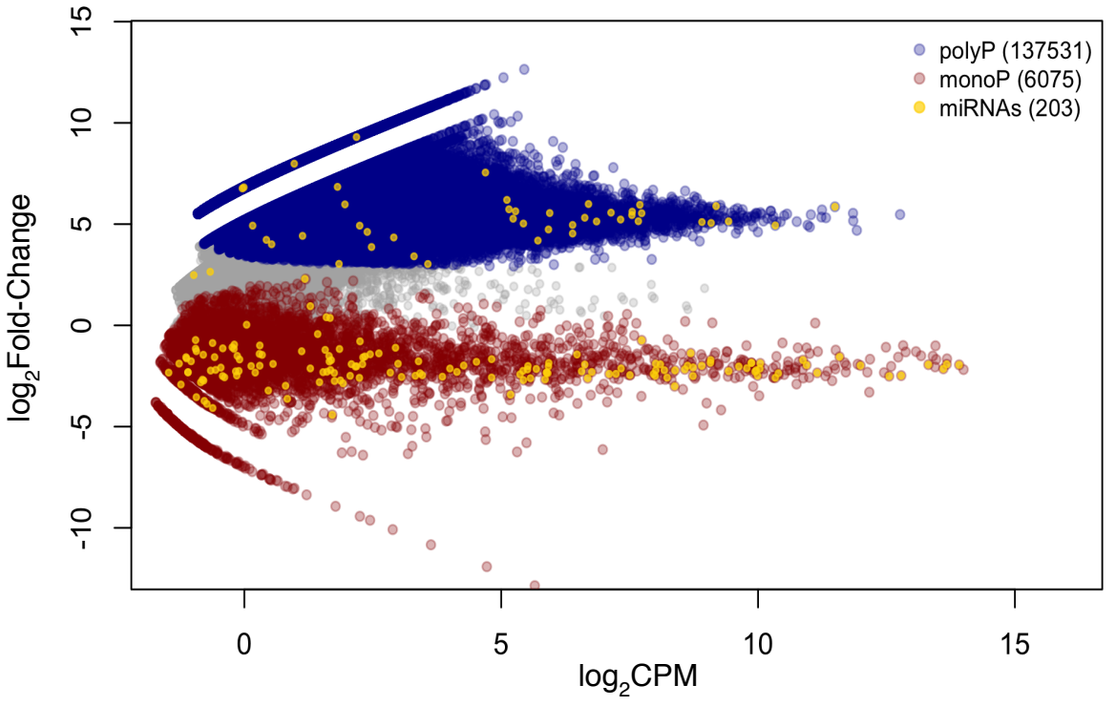

C) *H. bakeri* Vesicle libs, monoP and polyP-enriched clusters

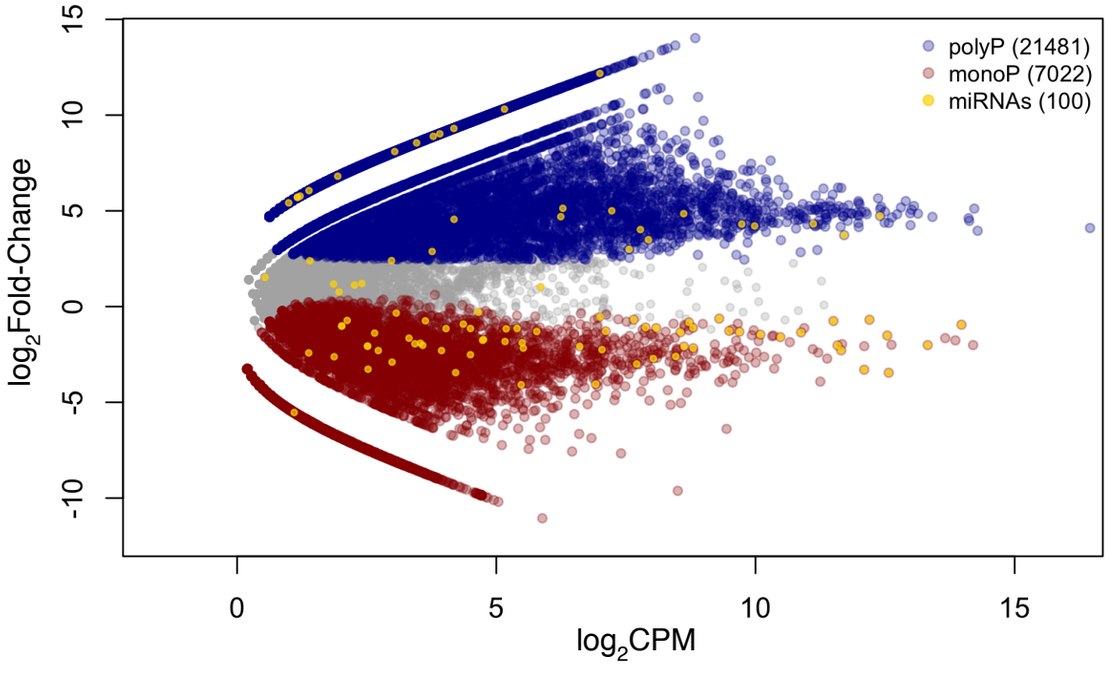

Supplemental Figure 3

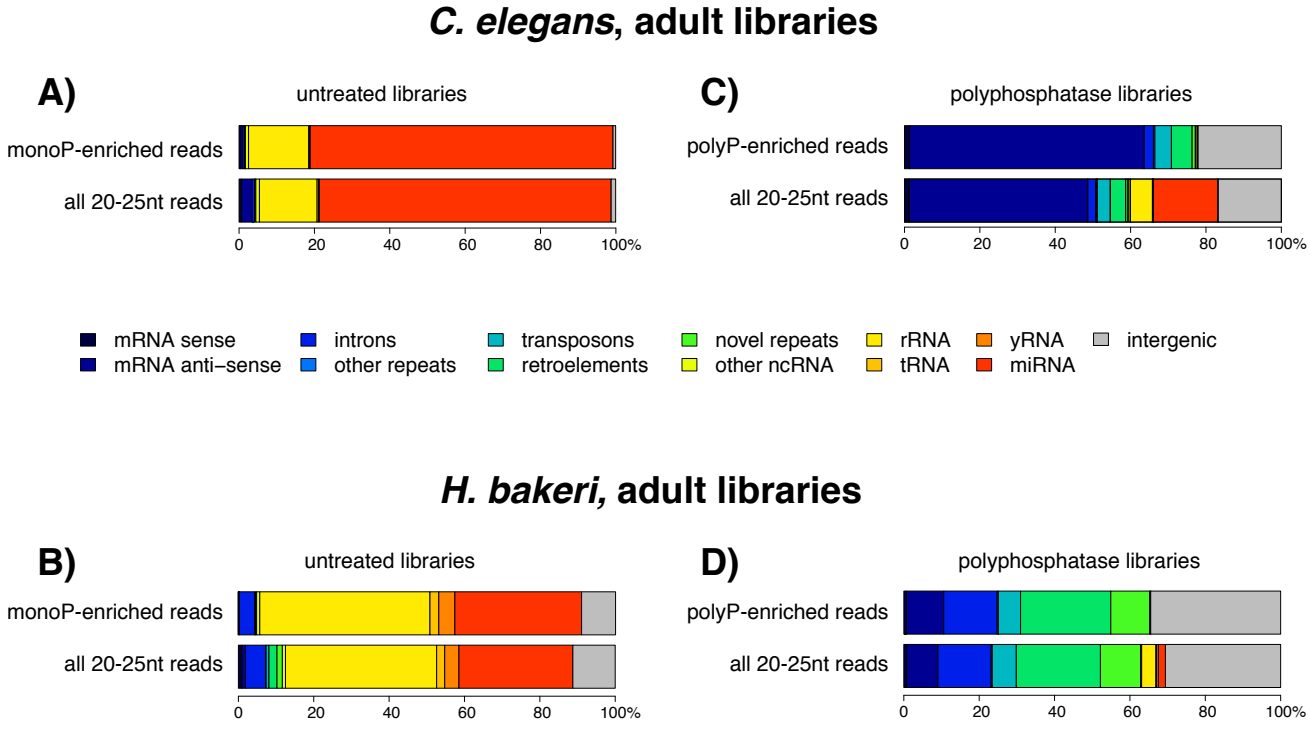

Supplemental Figure 4

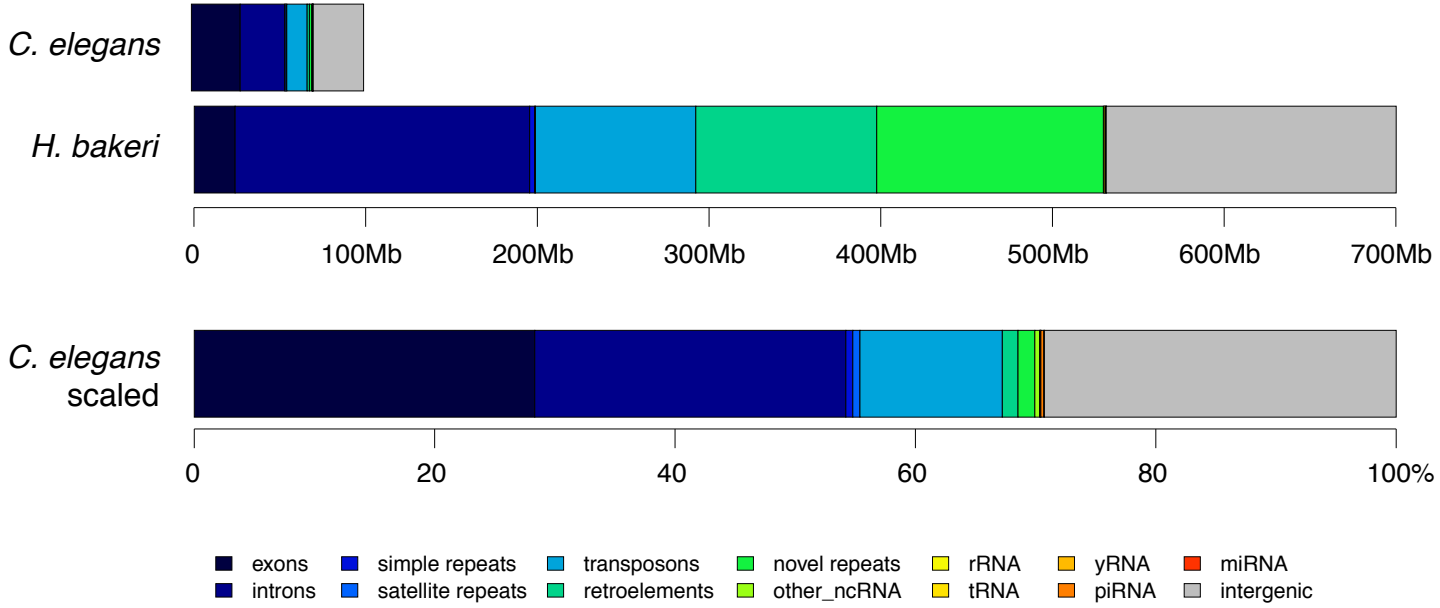

Supplemental Table 1: *Heligmosomoides bakeri* genome assembly

Feature	***Heligmosomoides bakeri* genome assembly v2.0**	***Heligmosomoides bakeri* genome assembly v1.0**
Reference	This work	WTSI
Span (Mb)	696	560
G+C content (%)	45.6	45.0
Scaffold / contig N50 (kb)	179.6 / 42.6	35.8 / 12.8
Number of contigs	23647	44728
Genome CEGMA complete / partial (%)	88.7 / 8.1	78.8 / 18.1
Genome BUSCO (Nematoda) complete / partial (%)	87.1 / 7.2	67.8 / 10.7
Genome BUSCO (Eukaryota) complete / partial (%)	87.8 / 1.7	74.3 / 8.9
Transcriptome mapping	96.3%	72.3%
Number of protein-coding genes	24371	27459